Published in final edited form as:
Neuropsychologia. 2009 January ; 47(1): 180–194. doi:10.1016/j.neuropsychologia.2008.08.011.

Reading impairment in a patient with missing arcuate fasciculus

Andreas M. Rauschecker[1,2], **Gayle K. Deutsch**[2], **Michal Ben-Shachar**[2], **Armin Schwartzman**[3], **Lee M. Perry**[2], and **Robert F. Dougherty**[2]

1 *Medical Scientist Training Program (MSTP) & Neurosciences Program, Stanford University School of Medicine, Stanford, CA*

2 *Psychology Department, Stanford University, Stanford, CA*

3 *Department of Biostatistics, Harvard University, Boston, MA*

Abstract

We describe the case of a child ("S") who was treated with radiation therapy at age 5 for a recurrent malignant brain tumor. Radiation successfully abolished the tumor but caused radiation-induced tissue necrosis, primarily affecting cerebral white matter. S was introduced to us at age 15 because of her profound dyslexia. We assessed cognitive abilities and performed diffusion tensor imaging (DTI) to measure cerebral white matter pathways. Diffuse white matter differences were evident in T1-weighted, T2-weighted, diffusion anisotropy, and mean diffusivity measures in S compared to a group of 28 normal female controls. In addition, we found specific white matter pathway deficits by comparing tensor orientation directions in S's brain with those of the control brains. While her principal diffusion direction maps appeared consistent with those of controls over most of the brain, there were tensor orientation abnormalities in the fiber tracts that form the superior longitudinal fasciculus (SLF) in both hemispheres. Tractography analysis indicated that the left and right arcuate fasciculus (AF), as well as other tracts within the SLF, were missing in S. Other major white matter tracts, such as the corticospinal and inferior occipitofrontal pathways, were intact. Functional MRI measurements indicated left-hemisphere dominanance for language with a normal activation pattern. Despite the left AF abnormality, S had preserved oral language with average sentence repetition skills. In addition to profound dyslexia, S exhibited visuospatial, calculation, and rapid naming deficits and was impaired in both auditory and spatial working memory. We propose that the reading and visuospatial deficits were due to the abnormal left and right SLF pathways, respectively. These results advance our understanding of the functional significance of the SLF and are the first to link radiation necrosis with selective damage to a specific set of fiber tracts.

> "Thus, printed letters of the alphabet, or words, signify certain sounds and certain articulatory movements. If the connection between the articulating or auditory centres, on the one hand, and the visual centres on the other, be ruptured, we ought *a priori* to expect that the sight of words would fail to awaken the idea of their sound, or the movement for pronouncing them. We ought, in short, to have alexia, or inability to read…"-William James, Principles of Psychology (1890)

Address for correspondence: Andreas M. Rauschecker, Psychology Department, Jordan Hall, 450 Serra Mall, Stanford, CA 94305-2130, Phone: 650-725-0051, Email: E-mail: andreasr@stanford.edu.

Introduction

Cranial irradiation is an effective treatment for primary and metastatic central nervous system tumors (e.g. Jenkin et al., 1998; Waber et al., 2001). However, it is well-known that long-term complications of radiation therapy can be severe, especially in children. Of the many types of damage, so-called late-delayed effects (including radiation necrosis) are the most devastating because of their irreversible nature. The pathophysiological mechanisms underlying this damage are an active area of research, and it is clear that the process is complex and involves damage to the endothelial cells of the vascular system and oligodendrocyte/astrocyte (O2-A) progenitor cells. [For a review, see Belka (2001) and Tofilon (2000)].

The cognitive consequences of radiation treatment are usually debilitating. In a longitudinal study of the effects of craniospinal irradiation on childhood medulloblastoma, significant reductions in IQ, reading, spelling, and math scores were reported, with reading skills especially affected in young patients (Mulhern et al., 2005). IQ changes are progressive, with a loss of 1.6 to 8.2 points per year (Fouladi et al., 2004; Mulhern et al., 2005). Other studies have demonstrated similar cognitive changes following radiation combined with chemotherapy (e.g. Fouladi et al., 2004; Mulhern et al., 2005; Reddick et al., 2006). Indeed, significant neuropsychological deficits are found in virtually all long-term survivors of childhood medulloblastoma treated with cranial irradiation (Walter et al., 1999).

Here we describe the case of a child (referred to as “S”) who was treated with whole-brain radiation therapy at age 5 for the recurrence of a malignant tumor in her upper spine and brain. The radiation treatment resulted in clinical remission, but left her with radiation-induced tissue necrosis, especially in the white matter of the brain. She was introduced to us at age 15 due to her extreme difficulties with learning to read. Damage produced as a result of radiation treatment is usually selective to white matter (Valk and Dillon, 1991), so we performed diffusion tensor imaging (DTI) to assess the state of white matter pathways and their connections in her brain. Most major white-matter pathways were intact in S, but she was missing much of the superior longitudinal fasciculus (SLF), a major set of connections between lateral-frontal language areas and language regions in the parietal and temporal lobes that include the arcuate fasciculus (AF). We further characterized her cognitive strengths and weaknesses with neuropsychological testing, and confirmed the location of key language regions using functional MRI.

Methods

Control Group

The control group was originally recruited for a longitudinal study of reading development. The data used here are from the first measurement in that longitudinal study. The group consisted of 54 children (25 males) ages 7–12 (median age 10.1). From this group we created two control groups; the first using the entire group of 54 and the second using only the 28 subjects who were female with basic reading scores greater than 90 (median age 9.7, range 7–12). Although results using either group as the control were virtually identical (compare Supplementary Figure 1 and Figure 3D), all data and figures presented here represent only the sex-matched control group, which does not include any children who meet the diagnostic criteria for dyslexia. All subjects were physically healthy and had no history of neurological disease, head injury, attention deficit/hyperactivity disorder, language disability, or psychiatric disorder. All subjects were native English speakers and had normal or corrected-to-normal vision and normal hearing. The Stanford Panel on Human Subjects in Medical and Non-Medical Research approved all procedures. Written informed consent/assent was obtained from all parents and children.

Although the control group used in this study is somewhat younger than the chronological age of S at the time of testing (15 years, 11 months), we believe that this group is representative of her developmental stage, due to her small physical stature and delayed puberty, which are a result of abnormal endocrine levels following radiation treatment. The brain undergoes major morphological changes during puberty (Sisk and Zehr 2005), and the interaction of delayed brain development and puberty may play a key role in learning problems (Wright and Zecker 2004); thus we believe that a younger control group provides the proper comparison for anatomical development in S. Furthermore, to rule out age as an explanation for the differences that we observe in S's brain, we also compared neurologically normal young adults to the younger control group. These subjects were recruited from the local community, also as part of a study of reading.

Subject S

Early Development—S's early development was reported to be normal. There is no history of learning disability, language disability or developmental delay in her family. Her mother reported that before her diagnosis S was able to identify most letters of the alphabet by sight and that she was beginning to read words and had a sight-word vocabulary of about 16 to 20 words. About one month after her fourth birthday, S was diagnosed with a primitive neuroectodermal tumor (PNET) in the C5 to C7 region of her spinal cord.

Treatment—Following surgical resection of the primary tumor and systemic chemotherapy, tumor cells were discovered in the cerebrospinal fluid. Intrathecal methotrexate chemotherapy only temporarily stopped the progression of the disease, leading to a full relapse less than a year after the tumor resection. Approximately 3 months before her fifth birthday, S received total neuraxis radiation treatment of 4080 rads, with a spinal boost to T5 (the largest tumor site of the relapse), for a total of 5040 rads. Doses of radiation were administered twice a day over the course of four weeks. Craniospinal radiation therapy resulted in immediate regression of the tumor but eventually led to late-delayed reactions, including frank radiation necrosis. Radiation treatment was followed by high-dose chemotherapy with stem-cell rescue as a precautionary measure.

Sequelae of Treatment—Although there has been no recurrence of the tumor, S has experienced other medical and cognitive complications. Secondary to spinal difficulties, she underwent an anterior and posterior spinal fusion soon after her seventh birthday. She had a halo placed when she was eight years of age, from which she developed an epidural hematoma in the right parietal area resulting in a coma of several hours. She then developed seizures and was medicated with phenytoin for a period of time. Medical reports indicate that "she recovered well from that episode, and there was no loss of skill that the family noted". She suffered some high-frequency hearing loss in her left ear following the epidural hematoma. S was monitored for several years with a series of annual follow-up MRIs to confirm that her condition was stable, as it remains today.

Growth and Physical Development—As a result of radiation treatment, S developed hypothalamic-pituitary hormonal dysfunction with resulting hypopituitarism, for which she has been treated since age 5 with the following medications: Synthroid (levothyroxine) for central hypothyroidism (since age 5), Humatrope (recombinant growth hormone) for growth hormone deficiency (since age 6), Cortef (hydrocortisone) for ACTH-cortisol insufficiency (since age 9 years, 7 months), Premarin (estrogen) for central hypogonadism (since age 14 years, 2 months), and Provera (progestin) for menstrual cycling (since age 14 years, 6 months).

All of the above conditions are a result of hypopituitarism related to radiation treatment, which has led to delayed physical development and decreased growth in S despite appropriate

medication. S has been below the 5th percentile in height and at approximately the 10th percentile in weight since treatment. At age 11 years, 8 months, X-rays showed a bone age of 10.5 years. S reached Tanner Stage 2 of thelarche (mean age 11 years, 1 month) at age 11, and Tanner Stage 2 of pubarche (mean age 11 years, 8 months) at age 13 years, 1 month. (See Marshall and Tanner (1969) for norms.)

At age 12 years, 6 months, she was diagnosed with “arrested pubertal development”. At age 14 years, 2 months, gonadotropin response to LHRH (leutinizing hormone releasing hormone) stimulation testing showed “dysregulation and disruption of the normal neuroendocrine pathways by her cranial irradiation”, and Premarin was started to replace normal production of gonadotropins. Onset of menses occurred with start of Provera at age 14 years, 5 months. In comparison, the average age of menarche in U.S. girls is 12 years, 5 months, with 90% of all US girls having undergone menarche by age 13 years, 9 months (Chumlea et al., 2003).

In summary, S has displayed delayed physical development and delayed puberty. Despite medications, S’s physical development has never fully recovered, being at the 5th–10th percentile in weight (43.5Kg) and less than the 5th percentile in height (136.5cm) at time of scanning. For comparison, her weight of 43.5Kg is typical of a 12–12.5 year-old, while her height of 136.5cm is typical of a 9.5–10 year old girl. [Norms from National Center for Health Statistics (2007)]. S’s head size was 3% larger than the average of our control group at the time of testing.

Education—Despite requiring these significant medical interventions, S did *not* miss a considerable amount of school. Her initial diagnosis occurred when she was 4 years of age. Therefore, her expected enrollment into a small private pre-school was delayed by one year, to the age of 5. She began kindergarten at 6 years of age, missing only four months at the end of kindergarten due to medical interventions. She started the 1st Grade the following year and completed the year without any interruption. The only other school interruption occurred in December of 2nd Grade but was limited to approximately three weeks around the winter break. From 2nd Grade until the present (S is currently in 11th Grade) there have been no interruptions in her educational experience. In summary, we would not expect her profound dyslexia and other cognitive deficits to be due to missing several months of kindergarten, although subtle effects cannot be ruled out.

White matter damage following radiation therapy was initially progressive, as was the development of large cystic regions in the left frontal and parietal lobes (compare Figures 1 and 2). S has also suffered several cognitive problems. Her most profound deficits are in reading acquisition and visuospatial processing, despite extensive reading remediation as well as math interventions. Since Kindergarten she has been in the public school system, and an Individual Education Program (IEP) allows for reading and math services during the day. She is in regular classes with an individual aide for all other subjects. S has undergone several speech and language screenings by the school district but never qualified for services.

S participated in the Lindamood-Bell® (LB®) Learning Processes (Lindamood-Bell, San Luis Obispo, CA) programs on multiple occasions. LB®’s programs are based on the premise that reading requires the integration of sensory-cognitive functions and skills. S received a combination of two of their programs: 1) LiPS® (Lindamood Phonemic Sequencing for Reading Spelling and Speech), which promotes phonemic awareness, and 2) Seeing Stars™ (Symbol Imagery for Sight Words, Reading, Phonemic Awareness, and Spelling), which targets word identification and reading fluency. In the fall of 1999, when S was in the 3rd grade, she had one semester of LB instruction 2 hours per day. By January of 2000 she had received 60 hours of LiPS® and 105 hours of SI™. In the summer of 2000, after 3rd grade, S attended an LB clinic 4 hours per day for 6 weeks and received a total of 58 hours of LiPS® and 58

hours of SI™. In the 8th grade (2004), she was administered LB for 2 hours per day for one semester and received 160 hours of SI™. In the 9th grade (2005), she was administered one year of LB for 2 hours each day, and received 310 hours of SI™. In the 10th grade, she received assistance with writing strategies by an LB consultant.

Pre- and post-testing of S's reading skills were assessed using the Gray Oral Reading Test-3 (GORT-3) (Widerholt and Bryant, 1994) and Gray Oral Reading Test-4 (GORT-4) (Wiederholt and Bryant, 2002), the Wide Range Achievement-Test-3 (WRAT-3) Reading subtest (Wilkinson, 1993), the Woodcock Reading Mastery Test-Revised (WRMT-R) (Woodcock, 1987) Word Attack subtest. Examining all reading scores it is evident that S demonstrated a flat learning curve based on her raw scores and a widening gap between her and same age peers over time based on her age corrected percentile scores (Table 1).

When S was in the 9th grade, her mother administered Read Naturally, a computerized reading fluency program (Ihnot et al., 2001). The participant practices reading the same stories multiple times with the goal of increasing reading speed. S practiced at the 1st grade level and improved her speed on average by 55 words per minute to 69 words per minute. The program is not designed to improve reading accuracy. There was no formal pre- and post-testing administered. In 10th grade she began a computerized math intervention program (Math Concepts and Skills 2) from SuccessMaker® Enterprise (Pearson Digital Learning, Pearson Education Inc., Phoenix, AZ) for one class per day; she also worked on it at night and on the weekends. The computer program started at the 3.0 grade level and was adjusted to the 3.5 grade level after administering a series of calculations to S. S spent approximately 83 hours on this program which covered computations (addition, division, multiplication, and subtraction) and applications (geometry, measurement, number concepts, probability and statistics, problem solving, science applications, word problems). By the end of the program S's cumulative performance was at the 4.87 grade level. There was no formal pre- and post-testing administered.

Past Neuropsychological Assessments—S is a right-handed female who was 15 years, 11 months at the time of our neuropsychological evaluation and DTI and fMRI scans. She had previously undergone neuropsychological evaluation at age 11 and a psycho-educational evaluation at age 13. These past assessments were notable for verbal abilities within the average range with significantly lower visuospatial and visuoperceptual skills, including well below average constructional skills. In these assessments there was no indication of difficulty with complex language comprehension, though speech was reported as "mildly dysnomic." More precise understanding of S's dysnomia is not known because no scores were listed in the report, but her dysnomia is not severe enough to be noticeable in normal conversation. Her memory was described as generally adequate with no marked distinction between verbal and visual memory. Problem-solving skills were reported to be within the average range. Her academic skills in reading and math were well below average. The neuropsychological assessment at age 11 was comprised of the following: Beery Test of Visuomotor Integration, Boston Naming Test, California Verbal Learning Test, three subtests (not specified in the report) of the Children's Memory Scale, Facial Recognition Test, Token Test, Rey Osterrieth Figure, the Wechsler Individual Achievement Test, and the Wechsler Intelligence Scale for Children-III (WISC-III). The only raw scores provided in the report of the neuropsychological evaluation were the WISC-III. All available test scores are presented in Table 2.

Neuropsychological Testing Procedures

Consent from the mother and assent from the child were obtained at the beginning of the study, consistent with the approved human subjects protocol by the Stanford Panel on Human Subjects in Medical Research.

Our neuropsychological evaluation of S consisted of the following measures: **Laterality**- Edinburgh Handedness Inventory (EHI); **Intellectual Functioning**- Wechsler Intelligence Scale for Children-IV (WISC-IV) (Wechsler, 2003); **Achievement**- Woodcock-Johnson Tests of Achievement-III (WJ-III) (Woodcock, 2001), the GORT-4 (Wiederholt and Bryant, 2002), Test of Word Reading Efficiency (TOWRE) (Torgesen, 1999); **Phonological Processing**- Comprehensive Test of Phonological Processing (CTOPP) (Wagner et al., 1997); **Language**- Clinical Evaluation of Language Fundamentals-4 (CELF-4) (Semel, 2003), Controlled Oral Word Association Test, Animal Naming Test, Boston Naming Test-2 (Kaplan, 2001); **Executive Function**- Wisconsin Card Sorting Test (Heaton, 1993); **Memory**- Wechsler Memory Scale-III (Wechsler, 1997).

Imaging methods: DTI

Diffusion-weighted imaging (DWI) data were acquired on a 1.5T Signa LX (Signa CVi, GE Medical Systems, Milwaukee, WI) using a self-shielded, high performance gradient system capable of providing a maximum gradient strength of 50mT/m at a gradient rise time of 268μs for each of the gradient axes. A standard quadrature head coil, provided by the vendor, was used for excitation and signal reception. Head motion was minimized by placing cushions around the head and securing a Velcro strap across the forehead.

The DWI protocol used eight 90-second whole-brain scans; these were averaged to improve signal quality. The pulse sequence was a diffusion-weighted single-shot spin-echo, echo planar imaging sequence (TE =63ms; TR = 6s; FOV = 260 × 260 mm; acquisition and reconstruction matrix size = 128 × 128; bandwidth = ±110kHz; partial k-space acquisition). We acquired 56 axial, 2 mm thick slices (no skip) for b = 0 and b = 800 s/mm^2. The higher b-value was obtained by applying gradients along 12 different diffusion directions (six non-colinear directions). Two gradient axes were energized simultaneously to minimize TE. The polarity of the effective diffusion-weighting gradients was reversed for odd repetitions.

DTI data were pre-processed using a custom program that removed eddy current distortion effects and determined a constrained non-rigid image registration using normalized mutual information (Bammer et al., 2001). The six elements of the diffusion tensor were determined by multivariate regression (Basser, 1995; Basser and Pierpaoli, 1996). The eigenvalue decomposition of the diffusion tensor was also computed.

For each subject, the T2-weighted (b=0) images were coregistered to the corresponding T1-weighted 3D SPGR anatomical images. The coregistration was initiated using the scanner coordinates stored in the image headers to achieve an approximate alignment. This alignment was refined using a mutual-information 3D rigid-body coregistration algorithm from SPM2 (Friston and Ashburner, 2004). Several anatomical landmarks, including the anterior commissure (AC), the posterior commissure (PC) and the mid-sagittal plane, were identified by hand in the T1 images. With these landmarks, we computed a rigid-body transform from the native image space to the conventional AC-PC aligned space. The DTI data were then resampled to this AC-PC aligned space with 2 mm isotropic voxels using a spline-based tensor interpolation algorithm (Pajevic et al., 2002), taking care to rotate the tensors to preserve their orientation with respect to the anatomy (Alexander et al., 2001). The T1 images were resampled to AC-PC aligned space with 1 mm isotropic voxels. We confirmed by visual inspection of each dataset that this coregistration technique aligns the DTI and T1 images to within 1–2 millimeters in the brain regions of interest. However, geometric distortions inherent in EPI acquisition limit the accuracy in regions prone to susceptibility artifacts, such as orbito-frontal and anterior temporal regions.

We used standard non-linear spatial normalization methods from SPM2 to align the 54 control brains and build a template from them (see Dougherty et al., 2005). The diffusion data for

subject S had significant geometric distortions in the cerebellum and inferior occipital lobe due to the spinal fusion hardware in her neck. For this reason, we independently aligned her T1-weighted images and her DTI data to the control template brain. S's T1-weighted images were aligned to the control brain T1-weighted template. Her DTI data were normalized to this same coordinate space by aligning her non-diffusion-weighted EPI data to the template EPI. The resulting non-linear deformation was applied to the tensor field, taking care to rotate the tensors to preserve their orientation with respect to the anatomy by converting the local deformation field at each voxel to an affine transform and then applying the preservation of principal direction algorithm to the tensor at each voxel (Alexander et al., 2001).

The final result of these image manipulations produced a good alignment both between S's T1 and tensor data and between her brain and that of the 28 controls, as assessed by careful inspection. However, some severe artifacts due to the metal implants remained in the lower part of S's tensor data, especially in the cerebellum. Therefore, we restricted our analyses to the axial plane at or above the anterior commissure (Z>=0), which was about one centimeter above the artifact region.

Because we had suspected that certain pathways might be missing in subject S's brain, we did not want to compute the spatial normalization based on the diffusion-weighted data [e.g., using a method such as FSL's TBSS (Smith et al., 2006)]. Such methods are useful for finding diffusion differences between corresponding pathways but are not designed to find differences that might include the presence or absence of pathways.

Imaging methods: fMRI

We used an auditory covert verb generation paradigm to measure language related brain responses in S and identify her lateralization for language stimuli (Briellmann et al., 2006; Holland et al., 2001; Rowan et al., 2004). Auditory presentation was used to overcome S's reading difficulties (Szaflarski et al., 2006; Kipervasser et al., 2008). During the scans, S was asked to covertly generate verbs for each presented noun, and listen attentively to noise stimuli. We confirmed, using a short behavioral test, that S could perform the task overtly at a presentation rate of one word every three seconds. Experimental stimuli consisted of high frequency English nouns, presented aurally through MRI compatible headphones (Avotec, Inc., Stuart, FL). Control stimuli were auditory noise patterns created by randomizing the phase of the word stimuli, while maintaining their amplitude envelope. Each condition was repeated in six 15s blocks (consisting of 5 stimuli, ISI=3s) presented in pseudorandom order and interleaved with 15s rest periods. The whole experiment was divided into 2 short runs, 207s per run. Continuous MR data acquisition was used during these runs.

FMRI measurements were performed on a 3T General Electric scanner with a custom-built volume head coil. Head movements were minimized by padding and tape. Functional MR data were acquired with a spiral pulse sequence (Glover, 1999). Twenty-six oblique slices were prescribed approximately along the AC-PC plane, covering the whole temporal lobe and most of the frontal lobe (3 mm thick, no gap). The sampling rate of the BOLD signal (TR) was 3s and the voxel size was 2.5 × 2.5 × 3 mm.

In-plane anatomical images were acquired before the functional scans using a fast SPGR sequence. These T1-weighted slices were taken at the same location of the functional slices, and were used to align the functional data with the high-resolution T1 anatomical data acquired on the 1.5T scanner during the DTI scan session. The spiral sequence used for the fMRI was much less affected by the spinal fusion hardware in S's neck than the EPI-based DTI sequence, so no additional steps were necessary to obtain adequate alignment between the fMRI data and the subject's T1-weighted anatomical images.

FMRI data were analyzed using the freely-available mrVista tools (http://white.stanford.edu/software/). Images acquired from the functional scans were inspected for motion by an experienced analyst, who concluded that excessive motion in the second run (>5mm) was not corrected by our motion compensation procedure. Therefore the analysis was restricted to the first run. Our results thus rely on one functional run in which each condition was presented in 3 blocks. This is not uncommon in neurological patients and constitutes the main reason for using a powerful task that is known to activate language regions robustly even with very short scans (Kipervasser et al., 2008). Baseline drifts were removed from the time series by high pass temporal filtering. A small amount of spatial smoothing (with a 3 mm FWHM Gaussian kernel) was applied to the data to enhance sensitivity to small signal changes. A general linear model (GLM) was fit to each voxel's time course, estimating the relative contribution of each condition (verb generation, auditory noise) to the time course. GLM predictors were constructed as a boxcar for each condition convolved with a standard hemodynamic response model. Statistical maps were computed as voxel-wise t-tests for each predictor and between the weights of the two predictors. For visualization purposes, the statistical maps were interpolated to the high resolution volume anatomy.

Results

Cognitive functioning of S

S is strongly right-handed as assessed by the EHI [Laterality Index = 82] (Oldfield, 1971). She exhibited generally consistent intellectual abilities over the time she was formally evaluated, with relatively average verbal abilities and well below average visuospatial abilities (see Table 2). Her working memory abilities were well below average. Though the composite WMI from the WISC-IV is slightly different than the older version of the WISC-III's FD, the ability to hold auditory information in storage for a brief period was well below average. A similar level of impairment was observed on two tasks of phonological memory (i.e., repeating numbers and nonwords). In addition, spatial span was well below average. Processing speed was borderline deficient, which appeared to have fluctuated over time, but now the composite score for this domain is similar to the first assessment. She continues to show notable problems with all aspects of reading, including oral reading of single words and nonwords, as well as text comprehension. Although she is able to name letters, reading speed is very slow and she has difficulty understanding information that she reads. Reading ability is well below average (approximately at a second grade level). A written math test showed scores also falling well below average. S exhibited variable memory ability. Although her immediate recall of list items was well below average, her retention rate over 30 minutes is considered to be average, compared to same age peers. Immediate recognition memory for faces was average, whereas after 30 minutes it was below average. Conceptual reasoning, a component of executive functioning, was superior as assessed by a card-sorting test, suggesting that S's learning difficulties were not due to a diffuse global effect.

S performed well below average on all phonological processing measures (CTOPP). This included aural tests involving the ability to separate sounds of words (Elision), put sounds together to form words (Blending Words), repeat digit strings (Memory for Digits) and nonwords (Nonword Repetition), and quickly retrieve the names of letters (Rapid Letter Naming) and digits (Rapid Digit Naming).

S's cognitive functioning is notable for relatively spared oral language skills. Language testing involved measures of vocabulary, comprehension of aurally presented information, repetition of sentences, putting words together to form sentences, generating words, and confrontation naming. S's ability to repeat sentences within the average range is of particular interest given the missing left arcuate fasciculus (see below). It is also surprising given her below average auditory working memory. Although she exhibited weaknesses on a subtest of the CELF-4

(Semantic Relationships) and a measure of phonemic fluency (Controlled Oral Word Association Test), with both performances below average, her overall language abilities were within the average range. Some of the errors on the Semantic Relationship subtest involved problems with spatial associations, alphabetic sequencing, and temporal sequencing, so her below average performance can be attributed to impaired visuospatial abilities and the fact that she is unable to learn the alphabet. Likewise, difficulty with phonemic fluency but normal semantic fluency has been reported in individuals with dyslexia because of their inherent weakness relying on phonemic cues for access to the lexicon (Frith et al., 1995; Paulesu et al., 1996). It is also possible that auditory working memory difficulties contribute to low scores on the semantic relationships subtest of the CELF-4, and that although many of S's language performances are within the normal range, she may have difficulty with complex language concepts.

Diffuse white matter differences

A clinical MRI was performed on S at age 5 years, 10 months; that is, approximately nine months after completion of her radiation treatment. Axial slices from a T2-weighted spin-echo sequence are shown in Figure 1. The cystic regions had not yet formed at the time of this scan, but there is clear evidence of diffuse white matter differences. Our records indicate that the cysts were evident in subsequent clinical MRIs performed at age 7 years, 7 months (not shown). As is typical for radiation necrosis, the cysts and diffuse damage stabilized and persisted. The cystic regions and diffuse white matter pathology in subject S were apparent in all the scans that we performed at age 15 (see Fig 2). In particular, note the increased mean diffusivity (MD) and reduced fractional anisotropy (FA) in Figure 2, panels C and E. A control brain is shown in panels B, D and F for comparison. Based on these data and on previous studies showing treatment-induced FA differences (e.g. Leung et al., 2004), we expected her FA to be significantly reduced and her MD to be significantly elevated relative to the control brains in most of the white matter, and this was indeed the case (analysis not shown).

Tensor orientation differences

Diffuse, permanent white matter pathology likely indicates damage to the glia in the white matter (Belka et al., 2001; Nagesh et al., 2008). However, we also wanted to know if specific fiber pathways were morphologically different in S's brain. The principal diffusion direction (PDD) maps for S are shown in Figure 3A, the group-average PDD is shown in 3B, and a typical control PDD is shown in 3C. While S's PDD maps look relatively normal in most regions outside of the three cysts, we suspected differences in the region of the superior longitudinal fasciculus (SLF) based on preliminary inspection of the PDD maps.

To test for the possibility of missing or morphologically abnormal pathways, we performed a one-sample version of the tensor eigenvector test for tensor orientation differences described in Schwartzman (2006). This test compares the orientation of the frame of eigenvectors of the tensors in S's brain to the orientation of the frame of eigenvectors of the corresponding mean tensors in the control brains and produces a test statistic at each voxel. The p-values obtained from this statistic indicate the probability of obtaining a tensor orientation like that of S's brain from the distribution of the control-brain tensors at that same voxel. The results of this test are presented in Figure 3D. We controlled the expected value of the false discovery rate (FDR) such that no more than 5% of the statistically significant voxels in Figure 3D are expected to be false positives.

This analysis shows that in most regions of S's white matter, the tensor orientations (i.e. the eigenvectors) are *not* significantly different from those of the controls. However, several regions *were* significantly different from the control brains, including a large region in the vicinity of the SLF.

We checked the specificity of the tensor eigenvector orientation difference test by performing it on several individual brains (comparing them to the same control group) that were not part of the 28 control brains, including two young adults (one male and one female, both age 23) and two children (one male, age 8; one female, age 12). No differences were found, indicating that this test is sensitive only to major changes such as those seen in S, and not to normal individual variation.

We find that there is no change in our results when we compare S to a larger control group (n=54) that includes male subjects and individuals who meet criteria for dyslexia (Supplemental Figure 1). These findings are evidence that the abnormalities we observe in S's brain are not typical of poor readers; S's abnormalities in the SLF are much more drastic and qualitatively different from the more subtle white matter differences found in developmental dyslexia (see Discussion). In addition, our results are robust to the inclusion of male subjects in the control group. Our statistical test is conservative in the sense that it only unveils large tract orientation abnormalities. We stress that other methods would likely be needed for uncovering less drastic differences, such as those that are dependent on age, gender, or subtle anatomical abnormalities.

Tractography Analyses

To further understand the regions that showed significant differences in tensor orientation between S and the control group, we performed fiber tractography in S's brain and in the average of the control brains. While tractography through an average tensor map has been shown to be useful for visualizing the major white matter pathways (e.g., Catani et al., 2005), such analysis can miss many details. Therefore, we confirmed the average control brain tractography results presented below in several individual control brains (not shown).

Confirming the results of the tensor orientation difference test, tractography revealed that most major white matter pathways, including the corticospinal, inferior occipitofrontal, and a large parietofrontal pathway, are morphologically normal by visual inspection in S compared to control subjects (Fig 4). However, although the corticospinal pathway is present bilaterally in S (white in Fig 4A), it tends to bulge laterally (above the level of the internal capsule) when compared to this pathway in controls (compare white to purple in Fig 4A, Frontal View). This bulge is likely due to a displacement of these fibers to occupy an area that would normally contain the arcuate fasciculus, which is missing in S (see below). As a result, the tracts that now occupy this area in S have a different orientation than the normal SLF fibers in controls, and these changes are detected by the tensor orientation statistical analysis described above. It is important to note that we find no evidence of additional tracts; rather, existing normal tracts that still connect the same areas of the brain simply take a slightly more lateral course to their destinations. This bulge also caused a bilateral difference between S and the control group in the internal capsule, resulting in the statistical differences in the more inferior slices of Figure 3D. We believe the root cause of these internal capsule differences is the missing SLF pathways and thus we will focus subsequent analysis on those pathways. However, we must note the unlikely possibility that even if the cognitive changes were mostly due to the missing SLF pathways, the small differences in the paths of other tracts could play a role in S's difficulties. Moreover, we were unable to obtain reliable data below the level of the anterior commissure (Z=0) due to artifacts from spinal fusion hardware, so we cannot comment on possible differences in these inferior slices. There was one additional abnormal region in the right forceps major and adjacent gray matter. This region appeared to be due to a small misregistration between S's corpus callosum and the control group (the corpus callosum is particularly challenging to spatially normalize- see Dougherty, et al., 2005).

To explore the anatomical differences in S's brain, we intersected all white matter tracts in each hemisphere for S and controls with the statistically significant regions of diffusion tensor

orientation difference as regions of interest (ROIs). The differences in fibers passing through two of these ROIs between S and the control group are shown in Figure 5. Differences in the path of tracts seem to be due to the fact that large portions of the SLF, including the arcuate, are missing in S. The missing fibers lead to small but detectable differences in the location and direction of nearby fibers that are present in S, such as the left parietofrontal (Fig 5A) and right corticospinal (Fig 5B) fibers. Thus, when we overlap S's brain with the average of the control subjects, S's fibers look as if some of them have shifted into the areas surrounding the normal location of the SLF. As a result, different fiber pathways occupy the identified regions in S compared to controls. Importantly, these pathways are also present in controls, but their paths are slightly misplaced in S. The resulting differences in fiber orientation are illustrated by the mean diffusion ellipsoid insets of Figure 5,

The cystic regions in S's brain are also white matter regions with significant differences from the control group, so we performed a tractography analysis on the cystic regions to find the tracts that occupy the equivalent areas in the control group. In general, tracts that pass through these regions in controls are still present in S, passing around the outside of these cysts. However, one major U-fiber connection was discovered in controls that we were unable to locate in S. This pathway passes directly through the area now occupied by the CSF-filled cyst in the anterior region of S's left hemisphere (Figure 7B, yellow), and appears to connect middle-frontal gyrus with precentral gyrus in the controls. The functional significance of this loss is unknown. Notably, the control-brain SLF fibers that we were unable to locate in S do *not* pass through these cystic regions.

To confirm that the AF and the U-fibers described above were indeed missing in S, an expert searched manually for these tracts. This search was done at several levels of FA threshold, down to a very liberal threshold of 0.1 (which minimizes false negative fibers, but can increase false positives). For the AF, a coronal plane in each hemisphere was defined approximately half way between the posterior temporal lobe and the inferior frontal gyrus. Since the AF would need to cross through this plane, we narrowed our search of white matter tracts to those intersecting this plane. All remaining fibers were grouped into tracts that connect distinct regions of the brain. Only one of these fiber tracts was found to resemble the left arcuate in S, connecting the temporal lobe to a part of ventral premotor cortex (white fibers in Figure 7A). Although this tract resembles the shape of the arcuate, it does *not* connect to the cortical regions expected for the arcuate, such as the left inferior frontal gyrus. The left inferior frontal gyrus was functionally confirmed as Broca's area in S using fMRI, as described below, yet no identifiable long-range connections reached this ROI.

To examine the possibility of functional cortical reorganization, S performed a verb generation task during a BOLD fMRI session. This procedure allowed us to confirm the location of S's Broca's area in the left inferior frontal gyrus. Moreover, the pattern of activation in S clearly suggests left lateralization for language, matching the common patterns found in the healthy population of adults and children (Holland et al., 2001). Figure 6 shows the statistical maps for the verb generation condition (Figure 6A) and the auditory control condition (Figure 6B). Verb generation engaged well-known language areas in the left hemisphere including left inferior frontal gyrus and anterior insula (in Broca's area, point of maximal activation in Talairach coordinates: [−40, 14, 10].), and left posterior superior temporal gyrus (in Wernicke's area, point of maximal activation in Talairach coordinates: [−58, −50, 4]). Auditory noise stimuli activated the auditory cortex bilaterally (Figure 6B).

We placed S's functionally defined Broca's area in the same coordinate frame as her DTI data and confirmed that the tract resembling the arcuate pathway shape in S does not reach as far anterior as her Broca's area (Figure 7A). In fact, these pathways appeared to enter cortex over 1 cm posterior to the most posterior part of the functionally defined Broca's area. In the right

hemisphere, no arcuate pathway was found, although this is less surprising given that this right hemisphere pathway is not universal among the general population.

To search for the missing U-fibers described above, we dilated the ROI encompassing the anterior cyst by several millimeters to ensure that the missing U-fibers were not simply displaced. We found several other tracts in controls that passed through the cyst ROI, and these tracts were present in S and generally surrounded the cyst, as if they have been pushed out of the way by the fluid-filled cyst in S. However, we did not find any evidence for S having the U-fibers shown in Figure 7B (yellow).

Discussion

Radiation can produce damage to specific pathways

Our results indicate that damage from radiation-induced white matter necrosis can be both diffuse and focal. In previous studies of radiation-induced white matter necrosis, diffuse changes in fractional anisotropy (FA) and mean diffusivity (MD) due to radiation treatment have been shown to correlate with decreasing IQ (Khong et al., 2006; Mabbott et al., 2006). In this study, we propose that more specific cognitive deficits may be linked to acute damage to particular fiber tracts, such as the arcuate fasciculus (AF). As in similar cases, S presents with diffuse white matter differences in T1- and T2-weighting as well as diffusion (e.g. Chan et al., 2003; Khong et al., 2003). Such diffuse changes likely caused some of the global cognitive deficits that we see in S. Yet, despite these diffuse changes, our results suggest that the majority of fascicles appear to be morphologically intact and show a normal pattern of connectivity in most regions. Thus, although all white matter may be affected in some common way by radiation, the regional connectivity is largely preserved. Chemotherapy, although not emphasized here because of its uncertain effects, may also have a global impact on cerebral white matter pathology (Asato et al., 1992), especially when used in combination with radiation treatment (Fouladi et al., 2004; Reddick et al., 2006). In contrast to such global pathology that would be expected to cause global cognitive deficits, several specific tracts, including those comprising large portions of the superior longitudinal fasciculus (SLF), are missing in S. In some parts of the white matter, the missing tracts left CSF-filled cysts, but in most other parts, neighboring normal tracts filled the void. Thus, cysts do not necessarily signify missing tracts in white matter. Because of this, it would be difficult if not impossible to estimate which fascicles are abnormal without using diffusion MR and tractography. We hypothesize based on our findings in a single patient that specific cognitive deficits, such as reading problems, may be caused by the loss of specific white matter pathways following radiation treatment. Future studies should test this hypothesis in a larger group of patients.

Functions of the Arcuate Fasciculus

The results of this paper support the idea that at least some cases of alexia can be explained by a disconnectionist account (Epelbaum et al., 2008), since radiation treatment primarily affects white matter. Indeed, the most striking feature of S's brain is the missing AF in both hemispheres (Figure 7). While the diffuse white matter differences would be expected to produce some cognitive deficits, it is tempting to attribute S's profound reading deficit to the particular damage to the missing AF fibers, as this pathway connects regions crucial to language, including Broca's and Wernicke's areas, and is thought to be critical for proficient language and reading.

Acute lesions of the left arcuate are traditionally thought to produce a conduction aphasia evidenced by phonemic paraphasias and a reduced ability to repeat sentences, but with intact language comprehension and fluent speech (Damasio and Damasio, 1980). Despite the missing AF, S has relatively normal oral language in general and an average ability to repeat sentences.

Thus, S does not exhibit a conduction aphasia. Other studies have shown intact sentence repetition with lesions of the AF (Selnes, 2002; Shuren et al., 1995). This case provides additional evidence that the ability to repeat sentences is not necessarily dependent on the AF.

Functions associated with the AF in the dominant (left) hemisphere have been proposed for many years, but less is known about the homologous pathway in the right hemisphere. One section of the right AF near the inferior parietal lobe may be associated with visuospatial processing (Barrick et al., 2007; Buchel et al., 2004), a domain in which S has extreme difficulty. Though the relationship between reading and the right AF has not been systematically studied, there is evidence from lesion and imaging studies that the right hemisphere may play a role in orthographic processing (Tagamets et al., 2000), as well as providing a compensatory role in dyslexic readers (Coltheart, 2000; Shaywitz et al., 2006; Simos et al., 2007). Considering that S is missing all segments of the AF in both hemispheres, we speculate that these losses may be related to her poor performances in reading, visuospatial processing, and working memory capabilities for both auditory and spatial information. S's problems are not limited to reading, and it is likely that the diffuse white matter damage seen on T1 and T2-weighted MRI contribute to her global cognitive deficits.

DTI has allowed us to discover more focal anatomical abnormalities in the SLF, including an absent AF, that go beyond the diffuse damage seen with conventional MRI. Given that reading, working memory, and visuospatial skills are relatively more impaired compared to other cognitive tasks such as language, processing speed, and verbal memory, we think that these particular impairments may be best explained by the focal anatomical abnormalities. Precise parceling out of the abnormalities and their effects on S's reading is not possible given the retrospective design of the study, but discussion of some of her cognitive impairments in the context of her reading problems is warranted. A broad model of reading (Wagner, Torgesen & Rashotte, 1999) postulates that phonological awareness, phonological memory, and rapid naming contribute to the ability to skilled reading. An association has been made among impaired phonological awareness and impaired automaticity retrieving names of digits, numbers, colors and objects and the ability to acquire reading skills. According to Wolf (1991; 1997) and Wolf and Bowers (1999) individuals with problems in both phonological awareness and rapid naming skills are considered to have a "double deficit" which is thought to be more resistant to reading interventions. This is compatible with S's history in that S has undergone extensive reading remediation but continues to have significant problems in reading. Although a missing AF is certainly not a requirement for double-deficit dyslexia, it is likely that the missing AF in S, as well as her more diffuse damage, have contributed to these profound deficits.

We do not believe that the differences in S's brain reported here are directly related to white matter differences in developmental dyslexia that have been reported recently. These reports show reduced FA in white matter regions in (Klingberg et al., 2000) or near (Beaulieu et al., 2005; Deutsch et al., 2005; Niogi et al., 2006) the AF. Those differences involved FA, which is a function of the eigenvalues, while the effects reported here involve the eigenvectors, or the orientation of fibers. When the principal diffusion direction (PDD), which is the first eigenvector, was directly tested in developmental dyslexia (Schwartzman 2006), no differences were found in the arcuate region, although subtle differences were found in more anterior regions. Another study of developmental dyslexia reported that poor readers may have additional interhemispheric connectivity (Dougherty et al., 2007). While the FA and PDD differences in developmental dyslexia are possibly due to subtle morphological differences between good and poor readers (Ben-Shachar et al., 2007), the differences reported here are much more radical and pervasive. It is clearly not the case that individuals with developmental dyslexia have missing AFs. Also, while we cannot rule out the possibility that S had

developmental dyslexia before her illness, this is not likely given the relatively low incidence of dyslexia and S's normal cognitive development before onset of treatment.

Moreover, while the association between the missing AF and profound dyslexia described here in S is suggestive, it is by no means conclusive. Given that S has suffered other medical problems, such as high frequency hearing loss due to an epidural hematoma of the right parietal region, this single case study cannot conclusively implicate the AF in the acquisition of reading skills. Medical records indicate that there were no changes in cognitive abilities following the hematoma. Thus the epidural hematoma and high frequency hearing loss cannot explain S's difficulties in learning to read, although we cannot say whether they may have added additional barriers to reading acquisition beyond those already present following radiation treatment.

The most striking anatomical abnormality is the loss of white matter pathways that we have identified, while the most striking functional abnormality to S and her family is her difficulty to learn to read. This correlation is remarkable, but due to the correlational nature of the study we cannot fully tease out whether the anatomical differences are a cause or a result of functional disturbances. We must acknowledge that some of the observed structural differences could be a result of differing levels of learning in S compared to controls (but see section on Why the SLF?), rather than being a cause of learning disabilities. Longitudinal DTI studies of patients with and without reading difficulties following radiation treatment should be performed to confirm or deny the suspicion that the AF is causally implicated in reading acquisition. Moreover, these studies will need to tease out the role of the direct and indirect arcuate pathways (Catani et al., 2005) in reading. Our results are nevertheless consistent with the specific hypothesis that loss of the AF can cause a pure alexia due to disconnection of the ventral reading system from perisylvian and anterior language areas (Epelbaum et al., 2008), especially since all segments (direct and indirect) of the left AF are missing in S (Fig 7A,B).

Why the SLF?

Curiously, the SLF seems to be the only major long-range connection severely affected by radiation treatment in S. One possible interpretation is that the SLF was one of the most actively developing pathways in S's brain when she underwent radiation therapy, and thus was the most severely affected of the major pathways. It is known that maturation of white matter continues throughout childhood and even into adulthood (Courchesne et al., 2000; Paus et al., 1999). Postmortem and structural MRI studies have provided evidence that the developmental course of white matter occurs in a caudal-rostral (inferior to superior and posterior to anterior) fashion with motor and sensory tracts developing before association fibers (for review, see Lenroot and Giedd, 2006). The AF has been visualized in infants between the ages of 1 and 4 months (Dubois et al., 2007), but it is not fully myelinated until later in life, around the second or third decade (Ashtari et al., 2007; Paus et al., 1999; Schmithorst et al., 2002; Yakovlev, 1967; Zhang et al., 2007). Paus et al. (2001; 1999) reported significant age-related changes in the density of the white matter in the left AF in 111 children ages 4 to 17 years. Since radiation treatment has a particularly destructive effect on oligodendrocyte progenitor cells (Belka et al., 2001; Panagiotakos et al., 2007; Schultheiss et al., 1995; Tofilon and Fike, 2000), it is plausible that this intervention may affect developing or undeveloped white matter most severely, since this tissue would have the highest requirement for progenitor cells.

An alternative explanation of the specificity of white matter loss would be that the dose of radiation was unevenly distributed throughout S's brain. While we were not witness to S's radiation treatments, nothing in her extensive records suggests that the radiation would have been particularly focused in the region of the brain where the AF resides. Also, the fact that homologous pathways were affected in both hemispheres argues against a dose-effect and in favor of the hypothesis that the arcuate is particularly vulnerable to radiation damage during childhood. Notably, at least one report indicates that regional susceptibility of white matter

damage (despite equal radiation doses across regions) does exist (Qiu et al., 2006). Longitudinal studies using radiation in developing animals may provide insights into this question of selective toxicity in the future. Knowledge about selective vulnerability to radiation at various stages of development would be critical information for patients and their physicians in allowing optimization of whole-brain as well as focal irradiation treatment strategies (e.g. modification of drug or radiation regimen as well as early neuropsychological intervention).

Advantage of DTI over conventional MRI

Damage produced as a result of radiation treatment is usually selective to white matter (Valk and Dillon, 1991); moreover, neurocognitive decline in patients with late-delayed effects is correlated with the severity of white matter lesions (Reddick et al., 2006). However, conventional MRI lacks the ability to detect early injury, during a period where it may still be reversible. DTI allows non-invasive visualization of white patter pathways and may therefore provide more specific and sensitive prognoses for patients. This possibility is especially pertinent given that changes in DTI measurements occur at an earlier stage than cognitive changes or changes seen with conventional MR (Khong et al., 2005). While traditional MRI can yield information about the general area of affected white matter (e.g., Palmer et al., 2002), DTI can be used to more precisely identify and characterize those pathways that are damaged.

Several recent studies have focused on using DTI in patients with radiation necrosis to measure decreases in FA. Mean FA across large regions of white matter has been shown to correlate with IQ (Khong et al., 2006; Mabbott et al., 2006), age of treatment, and deterioration of school performance (Khong et al., 2003; Khong et al., 2005). Differences in FA between radiation treatment patients and controls have also been measured on a voxel-wise basis (Leung et al., 2004), showing that regional decreases in FA are generally but not always correlated with radiation dose (Qiu et al., 2006).

Measuring FA allows the degree of directionality (i.e. anisotropy) of diffusion within white matter to be determined. However, this does not take into account the direction of diffusion. Using the tensor-orientation statistic, we quantitatively compared a single subject to a group of controls. By using diffusion tractography in conjunction with our statistical comparison of tensor orientation differences, we were able to identify specific tract abnormalities in an individual patient. This test is especially sensitive to the displacement of existing tracts- in this case due to the loss of neighboring tracts. Similar changes can also result from other pathologies, such as a brain tumor pushing fibers out of the way. Therefore, this analysis has a potentially wide array of medical applications.

Being able to draw inferences about an individual by comparing the individual's data to a group of controls is very meaningful. Ideally, our control group might have been more closely matched in age to S. However, comparing individual young adults to our control group, we have shown that our statistical test is not sensitive to changes that are dependent on age. Moreover, we stress that tractography results in S are independent of and therefore unaffected by the choice of control group.

Our findings provide a compelling anatomical account of S's dyslexia that is a result of earlier medical treatment. An explanation of the difficulties that burden individuals afflicted by cognitive problems has the potential to provide reassurance to those individuals and their families, as it has for S and her family. Therefore, an approach such as the one presented here, which provides probabilistic estimates of white matter abnormalities in an individual, can be highly valuable for patients in a clinical setting.

Conclusions

We have shown that it is possible to quantitatively compare white matter regions in a single subject with DTI data from a group of controls. Such a technique may prove very powerful in a clinical setting, where inferences made on a group level are less helpful than those made for an individual.

Our results demonstrate that in cases of radiation-induced necrosis, diffuse white matter differences evident in T2 and diffusion images may be accompanied by complete loss of specific pathways. The loss of large pathways may be evident in T2 images by cystic regions somewhere along the pathway, but as we have shown, this is not always the case. Careful analysis of the white matter using DTI combined with tractography is crucial for a more complete understanding of the changes caused by radiation-induced necrosis.

In the case of S, radiation and chemotherapy treatment resulted in some diffuse white matter damage, combined with loss of several tracts comprising the superior longitudinal fasciculus, including the arcuate pathway. This specific loss is an intriguing explanation for S's profound reading problems.

Supplementary Material

Refer to Web version on PubMed Central for supplementary material.

Acknowledgements

First and foremost we thank S for her willingness to share her story with us and her patient cooperation during our testing. S's courage and determination to overcome the challenges that she faced was deeply inspiring. We also thank S's mother for her extensive help in arranging the measurements, compiling medical records, and for her general persistence in seeing the project through. Brian Wandell provided guidance, Adele Behn performed neuropsychological testing, and Arvel Hernandez assisted with data collection and analysis. S's physicians and the imaging center where her clinical scans were performed provided films and digital files. We also thank Dr. Michael Greicius for comments on the manuscript.

References

Alexander DC, Pierpaoli C, Basser PJ, Gee JC. Spatial transformations of diffusion tensor magnetic resonance images. IEEE Trans Med Imaging 2001;20:1131–1139. [PubMed: 11700739]

Asato R, Akiyama Y, Ito M, Kubota M, Okumura R, Miki Y, Konishi J, Mikawa H. Nuclear magnetic resonance abnormalities of the cerebral white matter in children with acute lymphoblastic leukemia and malignant lymphoma during and after central nervous system prophylactic treatment with intrathecal methotrexate. Cancer 1992;70:1997–2004. [PubMed: 1525778]

Ashtari M, Cervellione KL, Hasan KM, Wu J, McIlree C, Kester H, Ardekani BA, Roofeh D, Szeszko PR, Kumra S. White matter development during late adolescence in healthy males: a cross-sectional diffusion tensor imaging study. Neuroimage 2007;35:501–510. [PubMed: 17258911]

Bammer R, Keeling SL, Augustin M, Pruessmann KP, Wolf R, Stollberger R, Hartung HP, Fazekas F. Improved diffusion-weighted single-shot echo-planar imaging (EPI) in stroke using sensitivity encoding (SENSE). Magn Reson Med 2001;46:548–554. [PubMed: 11550248]

Barrick TR, Lawes IN, Mackay CE, Clark CA. White matter pathway asymmetry underlies functional lateralization. Cereb Cortex 2007;17:591–598. [PubMed: 16627859]

Basser PJ. Inferring microstructural features and the physiological state of tissues from diffusion-weighted images. NMR Biomed 1995;8:333–344. [PubMed: 8739270]

Basser PJ, Pierpaoli C. Microstructural and physiological features of tissues elucidated by quantitative-diffusion-tensor MRI. J Magn Reson B 1996;111:209–219. [PubMed: 8661285]

Beaulieu C, Plewes C, Paulson LA, Roy D, Snook L, Concha L, Phillips L. Imaging brain connectivity in children with diverse reading ability. Neuroimage 2005;25:1266–1271. [PubMed: 15850744]

Belka C, Budach W, Kortmann RD, Bamberg M. Radiation induced CNS toxicity--molecular and cellular mechanisms. Br J Cancer 2001;85:1233–1239. [PubMed: 11720454]

Ben-Shachar M, Dougherty RF, Wandell BA. White matter pathways in reading. Curr Opin Neurobiol 2007;17:258–270. [PubMed: 17379499]

Briellmann RS, Labate A, Harvey AS, Saling MM, Sveller C, Lillywhite L, Abbott DF, Jackson GD. Is language lateralization in temporal lobe epilepsy patients related to the nature of the epileptogenic lesion? Epilepsia 2006;47:916–920. [PubMed: 16686657]

Buchel C, Raedler T, Sommer M, Sach M, Weiller C, Koch MA. White matter asymmetry in the human brain: a diffusion tensor MRI study. Cereb Cortex 2004;14:945–951. [PubMed: 15115737]

Catani M, Jones DK, ffytch DH. Perisylvian Language Networks of the Human Brain. Ann Neurol 2005;57:8–16. [PubMed: 15597383]

Chan YL, Yeung DK, Leung SF, Chan PN. Diffusion-weighted magnetic resonance imaging in radiation-induced cerebral necrosis. Apparent diffusion coefficient in lesion components. J Comput Assist Tomogr 2003;27:674–680. [PubMed: 14501357]

Chumlea WC, Shubert CM, Roche AF, Kulin HE, Lee PA, Himes JH, Sun SS. Age at Menarche and Racial Comparisons in US Girls. Pediatrics 2003;111:110–113. [PubMed: 12509562]

Coltheart M. Deep dyslexia is right-hemisphere reading. Brain Lang 2000;71:299–309. [PubMed: 10716863]

Courchesne E, Chisum HJ, Townsend J, Cowles A, Covington J, Egaas B, Harwood M, Hinds S, Press GA. Normal brain development and aging: quantitative analysis at in vivo MR imaging in healthy volunteers. Radiology 2000;216:672–682. [PubMed: 10966694]

Damasio H, Damasio AR. The anatomical basis of conduction aphasia. Brain 1980;103:337–350. [PubMed: 7397481]

Deutsch GK, Dougherty RF, Bammer R, Siok WT, Gabrieli JD, Wandell B. Children's reading performance is correlated with white matter structure measured by diffusion tensor imaging. Cortex 2005;41:354–363. [PubMed: 15871600]

Dougherty RF, Ben-Shachar M, Deutsch GK, Potanina P, Bammer R, Wandell BA. Occipital-callosal pathways in children: Validation and atlas development. Ann N Y Acad Sci 2005;1064:98–112. [PubMed: 16394151]

Dougherty RF, Ben-Shachar M, Deutsch GK, Hernandez A, Fox GR, Wandell BA. Temporal-callosal pathway diffusivity predicts phonological skills in children. Proc Natl Acad Sci USA 2007;104:8556–8561. [PubMed: 17483487]

Dubois J, Dehaene-Lambertz G, Perrin M, Mangin JF, Cointepas Y, Duchesnay E, Le Bihan D, Hertz-Pannier L. Asynchrony of the early maturation of white bundles in healthy infants: Quantitative landmarks revealed noninvasively by diffusion tensor imaging. Human Brain Mapping. 2007

Epelbaum S, Pinel P, Gaillard R, Delmaire C, Perrin M, Dupont S, Dehaene S, Cohen L. Pure alexia as a disconnection syndrome: New diffusion imaging evidence for an old concept. Cortex. 2008in press

Fouladi M, Chintagumpala M, Laningham FH, Ashley D, Kellie SJ, Langston JW, McCluggage CW, Woo S, Kocak M, Krull K, Kun LE, Mulhern RK, Gajjar A. White matter lesions detected by magnetic resonance imaging after radiotherapy and high-dose chemotherapy in children with medulloblastoma or primitive neuroectodermal tumor. J Clin Oncol 2004;22:4551–4560. [PubMed: 15542806]

Friston KJ, Ashburner J. Generative and recognition models for neuroanatomy. Neuroimage 2004;23:21–24. [PubMed: 15325348]

Frith CD, Friston KJ, Herold S, Silbersweig D, Fletcher P, Cahill C, Dolan RJ, Frackowiak RS, Liddle PF. Regional brain activity in chronic schizophrenic patients during the performance of a verbal fluency task. Br J Psychiatry 1995;167:343–349. [PubMed: 7496643]

Gathercole SE, Baddeley AD. Phonological memory deficits in language disordered children: Is there a causal connection? Journal of Memory and Language 1990;29:336–360.

Gathercole SE, Willis CS, Baddeley AD. Differentiating phonological memory and awareness of rhyme: Reading and vocabulary development in children. British Journal of Psychology 1991;82:387–406.

Glover GH. Simple analytic spiral K-space algorithm. Magn Reson Med 1999;42:412–415. [PubMed: 10440968]

Heaton, RK.; Chelune, GJ.; Talley, JL.; Kay, GG.; Curtis, G. Wisconsin Card Sorting Test (WCST) manual, revised and expanded. Psychological Assessment Resources; Odessa, FL: 1993.

Holland SK, Plante E, Weber Byars A, Strawsburg RH, Schmithorst VJ, Ball WS Jr. Normal fMRI brain activation patterns in children performing a verb generation task. Neuroimage 2001;14:837–843. [PubMed: 11554802]

Ihnot, C.; Mastoff, J.; Gavin, J.; Hendrickson, L. Read Naturally. St Paul, MN: Read Naturally; 2001.

Jenkin D, Danjoux C, Greenberg M. Subsequent quality of life for children irradiated for a brain tumor before age four years. Med Pediatr Oncol 1998;31:506–511. [PubMed: 9835903]

Kaplan, EF.; Goodglass, H.; Weintraub, S. The Boston Naming Test. Vol. 2. Lippincott Williams & Wilkins; Philadelphia: 2001.

Khong PL, Kwong DL, Chan GC, Sham JS, Chan FL, Ooi GC. Diffusion-tensor imaging for the detection and quantification of treatment-induced white matter injury in children with medulloblastoma: a pilot study. AJNR Am J Neuroradiol 2003;24:734–740. [PubMed: 12695214]

Khong PL, Leung LH, Chan GC, Kwong DL, Wong WH, Cao G, Ooi GC. White matter anisotropy in childhood medulloblastoma survivors: association with neurotoxicity risk factors. Radiology 2005;236:647–652. [PubMed: 16040920]

Khong PL, Leung LH, Fung AS, Fong DY, Qiu D, Kwong DL, Ooi GC, McAlanon G, Cao G, Chan GC. White matter anisotropy in post-treatment childhood cancer survivors: preliminary evidence of association with neurocognitive function. J Clin Oncol 2006;24:884–890. [PubMed: 16484697]

Kipervasser S, Palti D, Neufeld MY, Ben-Shachar M, Andelman F, Fried I, Korczyn AD, Hendler T. Possible remote functional reorganization in left temporal lobe epilepsy. Acta Neurol Scand 2008;117:324–331. [PubMed: 18005219]

Klingberg T, Hedehus M, Temple E, Salz T, Gabrieli JD, Moseley ME, Poldrack RA. Microstructure of temporo-parietal white matter as a basis for reading ability: evidence from diffusion tensor magnetic resonance imaging. Neuron 2000;25:493–500. [PubMed: 10719902]

Lenroot RK, Giedd JN. Brain development in children and adolescents: insights from anatomical magnetic resonance imaging. Neurosci Biobehav Rev 2006;30:718–729. [PubMed: 16887188]

Leung LH, Ooi GC, Kwong DL, Chan GC, Cao G, Khong PL. White-matter diffusion anisotropy after chemo-irradiation: a statistical parametric mapping study and histogram analysis. Neuroimage 2004;21:261–268. [PubMed: 14741664]

Mabbott DJ, Noseworthy MD, Bouffet E, Rockel C, Laughlin S. Diffusion tensor imaging of white matter after cranial radiation in children for medulloblastoma: correlation with IQ. Neuro Oncol 2006;8:244–252. [PubMed: 16723629]

Marshall WA, Tanner JM. Variations in pattern of pubertal changes in girls. Arch Dis Child 1969;44:291–303. [PubMed: 5785179]

Mulhern RK, Palmer SL, Merchant TE, Wallace D, Kocak M, Brouwers P, Krull K, Chintagumpala M, Stargatt R, Ashley DM, Tyc VL, Kun L, Boyett J, Gajjar A. Neurocognitive consequences of risk-adapted therapy for childhood medulloblastoma. J Clin Oncol 2005;23:5511–5519. [PubMed: 16110011]

Nagesh V, Tsien CI, Chenevert TL, Ross BD, Lawrence TS, Junick L, Cao Y. Radiation-induced changes in normal-appearing white matter in patients with cerebral tumors: A diffusion tensor imaging study. Int J Radiation Oncology Biol Phys 2008;70:1002–1010.

National Center for Health Statistics. U.S. Department of Health and Human Services; 2007. CDC Growth Charts: United States. http://www.cdc.gov/nchs/about/major/nhanes/growthcharts/charts.htm

Niogi SN, McCandliss BD. Left lateralized white matter microstructure accounts for individual differences in reading ability and disability. Neuropsychologia 2006;44:2178–2188. [PubMed: 16524602]

Oldfield RC. The assessment and analysis of handedness: The Edinburgh inventory. Neuropsychologia 1971;9:97–113. [PubMed: 5146491]

Pajevic S, Aldroubi A, Basser PJ. A continuous tensor field approximation of discrete DT-MRI data for extracting microstructural and architectural features of tissue. J Magn Reson 2002;154:85–100. [PubMed: 11820830]

Palmer SL, Reddick WE, Glass JO, Gajjar A, Goloubeva O, Mulhern RK. Decline in corpus callosum volume among pediatric patients with medulloblastoma: longitudinal MR imaging study. AJNR Am J Neuroradiol 2002;23:1088–1094. [PubMed: 12169462]

Panagiotakos G, Alshamy G, Chan B, Abrams R, Greenberg E, Saxena A, Bradbury M, Edgar M, Gutin P, Tabar V. Long-term impact of radiation on the stem cell and oligodendrocyte precursors in the brain. PLoS ONE 2007;2:e588. [PubMed: 17622341]

Paulesu E, Frith U, Snowling M, Gallagher A, Morton J, Frackowiak RS, Frith CD. Is developmental dyslexia a disconnection syndrome? Evidence from PET scanning. Brain 1996;119(Pt 1):143–157. [PubMed: 8624677]

Paus T, Collins DL, Evans AC, Leonard G, Pike B, Zijdenbos A. Maturation of white matter in the human brain: A review of magnetic resonance studies. Brain Research Bulletin 2001;54:255–266. [PubMed: 11287130]

Paus T, Zijdenbos A, Worsley K, Collins DL, Blumenthal J, Giedd JN, Rapoport JL, Evans AC. Structural maturation of neural pathways in children and adolescents: in vivo study. Science 1999;283:1908–1911. [PubMed: 10082463]

Qiu D, Leung LH, Kwong DL, Chan GC, Khong PL. Mapping radiation dose distribution on the fractional anisotropy map: applications in the assessment of treatment-induced white matter injury. Neuroimage 2006;31:109–115. [PubMed: 16448821]

Reddick WE, Shan ZY, Glass JO, Helton S, Xiong X, Wu S, Bonner MJ, Howard SC, Christensen R, Khan RB, Pui CH, Mulhern RK. Smaller white-matter volumes are associated with larger deficits in attention and learning among long-term survivors of acute lymphoblastic leukemia. Cancer 2006;106:941–949. [PubMed: 16411228]

Rowan A, Liegeois F, Vargha-Khadem F, Gadian D, Connelly A, Baldeweg T. Cortical lateralization during verb generation: a combined ERP and fMRI study. Neuroimage 2004;22:665–675. [PubMed: 15193595]

Schmithorst VJ, Wilke M, Dardzinski BJ, Holland SK. Correlation of white matter diffusivity and anisotropy with age during childhood and adolescence: a cross-sectional diffusion-tensor MR imaging study. Radiology 2002;222:212–218. [PubMed: 11756728]

Schultheiss TE, Kun LE, Ang KK, Stephens LC. Radiation response of the central nervous system. Int J Radiat Oncol Biol Phys 1995;31:1093–1112. [PubMed: 7677836]

Schwartzman, A. Thesis. Stanford University; Stanford: 2006. Random ellipsoids and false discovery rates: statistics for diffusion tensor imaging data.

Selnes OA, van Zijl PCM, Barber PB, Hillis AE, Mori S. MR diffusion tensor imaging documented arcuate fasiculus lesion in a patient with normal repetition performance. Aphasiology 2002;16:897–901.

Semel, EM.; Wiig, EH.; Secord, WA. Clinical Evaluation of Language Fundamentals-Fourth Edition. PsychCorp; San Antonio: 2003.

Shaywitz BA, Lyon GR, Shaywitz SE. The role of functional magnetic resonance imaging in understanding reading and dyslexia. Dev Neuropsychol 2006;30:613–632. [PubMed: 16925477]

Shuren JE, Schefft BK, Yeh HS, Privitera MD, Cahill WT, Houston W. Repetition and the arcuate fasciculus. J Neurol 1995;242:596–598. [PubMed: 8551322]

Simos PG, Fletcher JM, Sarkari S, Billingsley-Marshall R, Denton CA, Papanicolaou AC. Intensive instruction affects brain magnetic activity associated with oral reading in children with persistent reading disabilities. Journal of Learning Disabilities 2007;40:37–48. [PubMed: 17274546]

Sisk CL, Zehr JL. Pubertal hormones organize the adolescent brain and behavior. Frontiers in Neuroendocrinology 2005;26:163–174. [PubMed: 16309736]

Szaflarski JP, Schmithorst VJ, Altaye M, Byars AW, Ret J, Plante E, Holland SK. A longitudinal functional magnetic resonance imaging study of language development in children 5 to 11 years old. Ann Neurol 2006;59(5):796–807. [PubMed: 16498622]

Smith SM, Jenkinson M, Johansen-Berg H, Rueckert D, Nichols TE, Mackay CE, Watkins KE, Ciccarelli O, Cader MZ, Matthews PM, Behrens TE. Tract-based spatial statistics: voxelwise analysis of multi-subject diffusion data. Neuroimage 2006;31:1487–1505. [PubMed: 16624579]

Tagamets MA, Novick JM, Chalmers ML, Friedman RB. A parametric approach to orthographic processing in the brain: an fMRI study. J Cogn Neurosci 2000;12:281–297. [PubMed: 10771412]

Tofilon PJ, Fike JR. The radioresponse of the central nervous system: a dynamic process. Radiat Res 2000;153:357–370. [PubMed: 10798963]

Torgesen, JK.; Wagner, RK.; Rashotte, CA. Test of Word Reading Efficiency. Pro-Ed; Texas: 1999.

Valk PE, Dillon WP. Radiation injury of the brain. AJNR Am J Neuroradiol 1991;12:45–62. [PubMed: 7502957]

Waber DP, Shapiro BL, Carpentieri SC, Gelber RD, Zou G, Dufresne A, Romero I, Tarbell NJ, Silverman LB, Sallan SE. Excellent therapeutic efficacy and minimal late neurotoxicity in children treated with 18 grays of cranial radiation therapy for high-risk acute lymphoblastic leukemia: a 7-year follow-up study of the Dana-Farber Cancer Institute Consortium Protocol 87–01. Cancer 2001;92:15–22. [PubMed: 11443604]

Wagner, RK.; Torgesen, JK.; Rashotte, CA. Comprehensive Test of Phonological Processing. Pro-Ed; Incorporated, Austin, TX: 1997.

Walter AW, Mulhern RK, Gajjar A, Heideman RL, Reardon D, Sanford RA, Xiong X, Kun LE. Survival and neurodevelopmental outcome of young children with medulloblastoma at St Jude Children's Research Hospital. J Clin Oncol 1999;17:3720–3728. [PubMed: 10577843]

Wechsler, D. WMS-III Administration and Scoring Manual. The Psychological Corporation; San Antonio: 1997.

Wechsler, D. Wechsler Intelligence Scale for Children-Fourth Edition. Vol. 4. PsychCorp; San Antonio: 2003.

Wiederholt, JL.; Bryant, BB. Gray Oral Reading Tests-Third Edition. Pro-Ed; Austin, TX: 1994.

Wiederholt, JL.; Bryant, BB. Gray Oral Reading Tests. Vol. 4. Pro-Ed; Austin, TX: 2002.

Wilkinson, GS. Wide Range Achievement Test 3. Wilmington, DE: Wide Range, Inc; 1993.

Wolf M. Naming speed and reading: The contribution of the cognitive neurosciences. Reading Research Quarterly 1991;26:123–141.

Wolf, M. A provisional, integrative account of phonological and naming-speed deficits in dyslexia: Implications for diagnosis and intervention. In: Blachman, B., editor. Foundations of reading acquisition and dyslexia. Philadelphia: Lawrence Erlbaum Associates; 1997. p. 67-92.

Wolf M, Bowers P. The "Double-Deficit Hypothesis" for the developmental dyslexias. Journal of Educational Psychology 1999;91:1–24.

Woodcock, RW. Woodcock Reading Mastery Tests-Revised. Circle Pines, MN: American Guidance Service; 1987.

Woodcock, RW.; McGrew, KS.; Mather, N. Woodcock-Johnson-III Tests of Achievement. Riverside Publishing; Itasca, IL: 2001.

Wright BA, Zecker SG. Learning problems, delayed development, and puberty. Proc Natl Acad Sci USA 2004;101:9942–9946. [PubMed: 15210987]

Yakovlev, PI. Regional development of the brain in early life. Blackwell Scientific; Oxford: 1967.

Zhang J, Evans A, Hermoye L, Lee SK, Wakana S, Zhang W, Donohue P, Miller MI, Huang H, Wang X, van Zijl PC, Mori S. Evidence of slow maturation of the superior longitudinal fasciculus in early childhood by diffusion tensor imaging. Neuroimage 2007;38:239–247. [PubMed: 17826183]

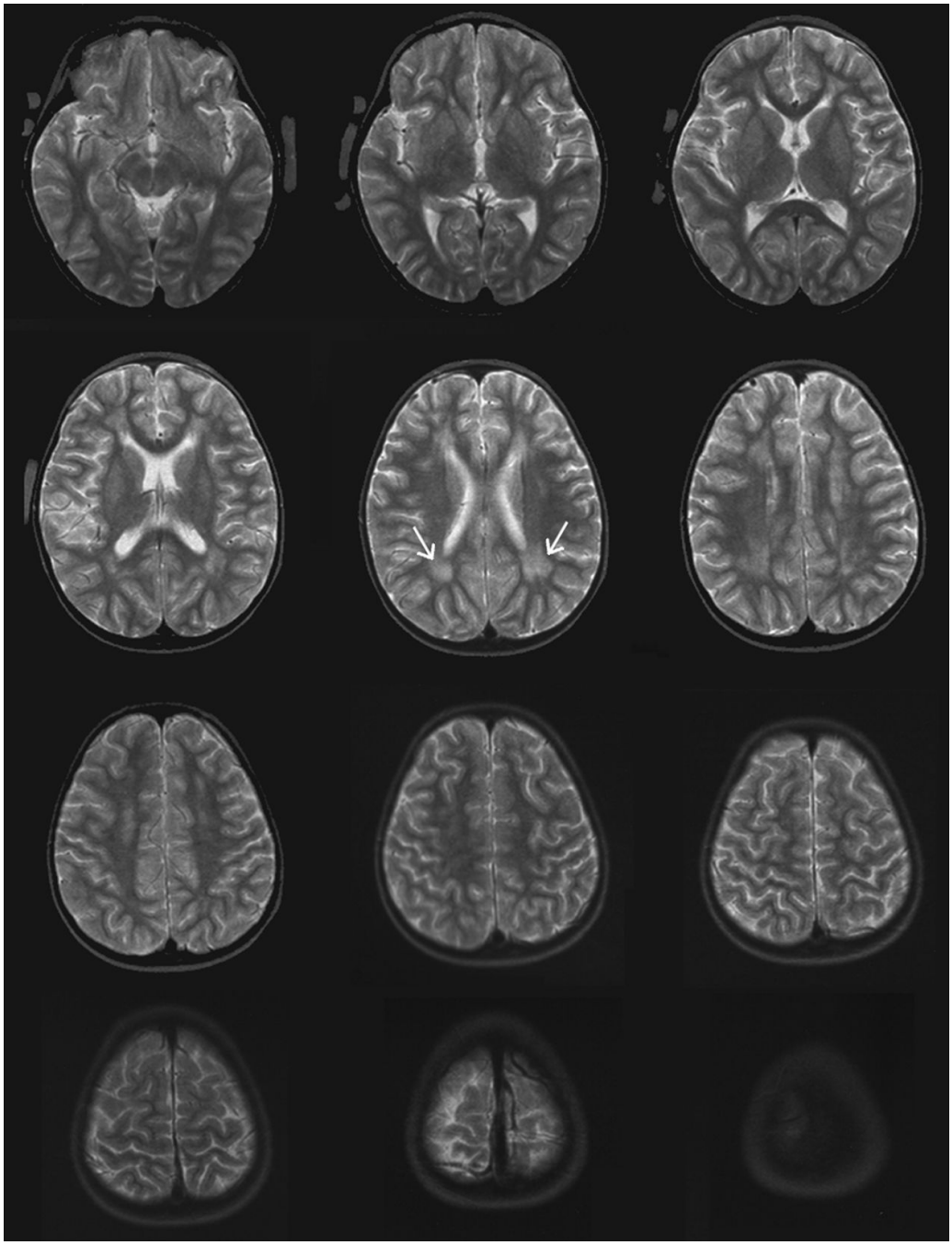

Figure 1.
T2-weighted scans from S at age 5, shortly after completion of radiation therapy (slices are approximately Z=0 through Z=60). The cystic lesions had not formed by this time, but regions of white matter damage are evident (white arrows).

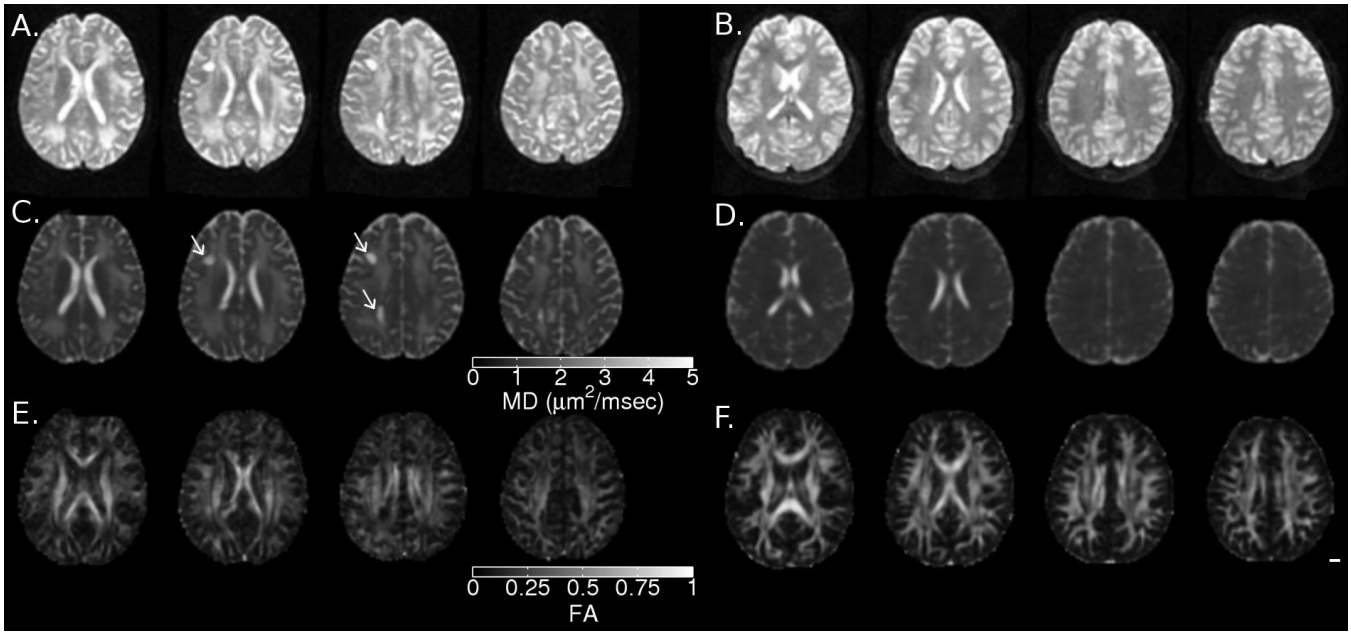

Figure 2.

Axial slices (Z=20, 25, 30 and 35) showing T2-weighted (A, B), mean diffusivity (C, D) and fractional anisotropy (E, F) for S (A, C, E) and a 12 year old female control subject (B, D, F). The two large cystic lesions in the left hemisphere are evident in A and C (arrows). Diffusely increased mean diffusivity (MD) and reduced fractional anisotropy (FA) are evident in panels C and E, respectively.

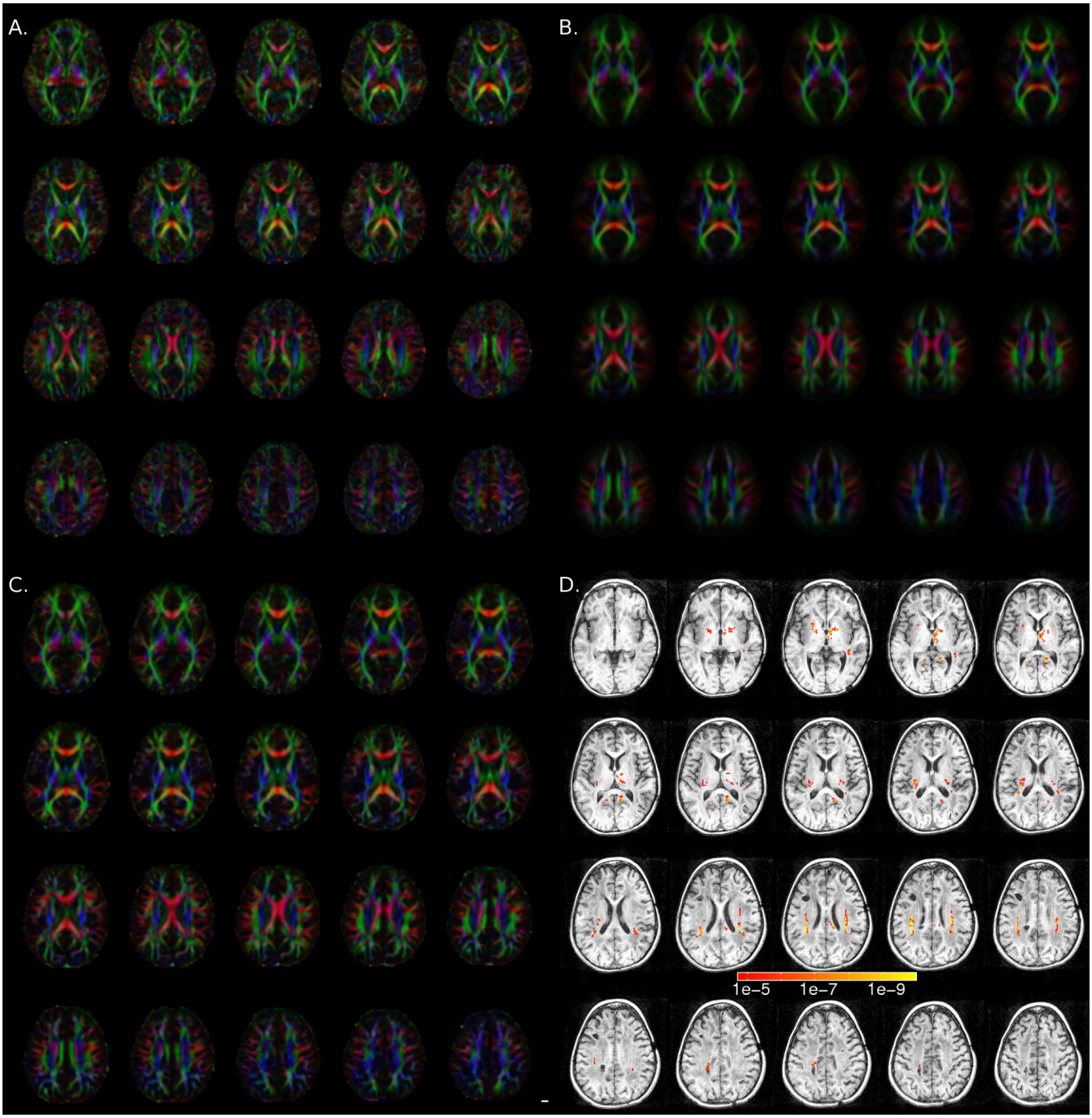

Figure 3.

Tensor orientation differences. (A–C) Axial slices (Z=2 through Z=40) showing principal diffusion direction (PDD) maps, where red indicates a left-right fiber orientation, green an anterior-posterior orientation and blue a superior-inferior orientation. (A) subject S, (B) control group average, and (C) control subject (12 year old girl). In (B) and (C), the brightness is modulated by the fractional anisotropy (FA), in (A), the brightness is modulated by 1.2*FA to account for S's overall reduction in FA. Panel (D) shows the results from the log-tensor one-sample eigenvector difference test (S vs. 28 controls) overlayed on a montage of S's T1-weighted image. Colorbar legend represents p values. Only voxels with $p<10^{-4.7}$ are shown (FDR = 5%, cluster threshold of 10 voxels).

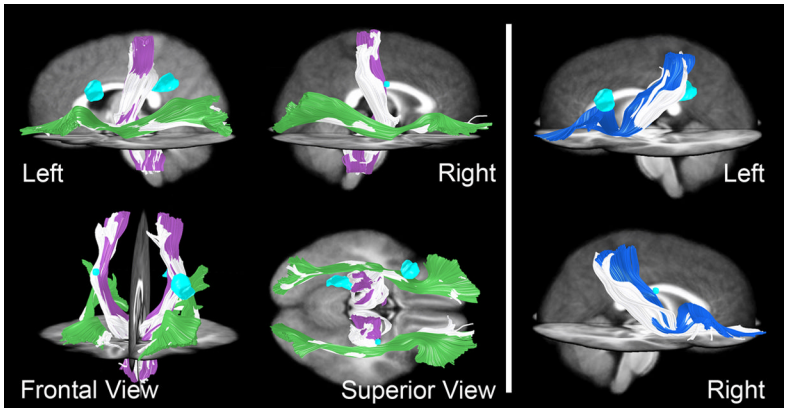

Figure 4.
Tractography of normal pathways in S (white) and 28 controls (colored). (A) Corticospinal (purple in controls) and inferior occipitofrontal pathways (green in controls) were relatively normal in S compared to the control group. (B) Parietofrontal pathways (blue in controls) were also spared. Cyan-colored regions represent cystic regions in S's brain.

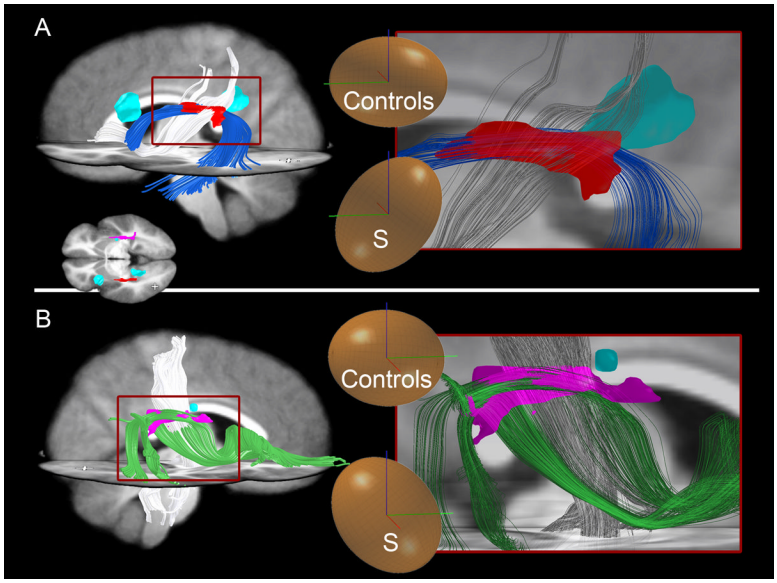

Figure 5.

Two examples of areas identified by our statistical test (Fig 3D) that contain different pathways in S than in controls, as shown by tractography. To explain why we found statistical differences in fiber orientation, we used tractography to visualize, in S and in controls, the fibers passing through the regions of interest (ROIs) created by the statistical test. Two ROIs are shown here in red (A) and violet (B), transformed into 3D from Fig 3D. Normal fibers in S take a path through the void created by missing SLF fibers. Blue (A) and green (B) fibers are SLF fibers present in controls that were subsequently shown to be absent in S. Instead, other fibers (displayed in white) course through the same areas in S. Note that for clarity, pathways shown are the major pathways passing through the ROIs but do not encompass all fibers through these areas. (A) In controls, the major pathway passing through the ROI (red) is the classical arcuate pathway (blue), while in S, the major pathway through this area connects the parietal and frontal cortices (white). In controls, this parietofrontal pathway is located more medial (not shown in figure). (B) In controls, a part of the SLF connecting temporal to frontal lobes (green) passes through the ROI, while in S, the corticospinal tract (white) is the major pathway passing through here. In controls, the corticospinal pathway is located more medial (not shown in figure). Inset on bottom left in panel A shows superior view of an axial slice with location of ROIs (red and violet) and cysts (cyan-colored). Insets on right panels show diffusion tensor ellipsoids of S and control group within each ROI. Roughly, ellipsoids indicate the probability of diffusion in each direction within that ROI. Note the difference in principal axis direction of these ellipsoids between S and controls. Bars in ellipsoids: green=anterior, blue=superior, red=right.

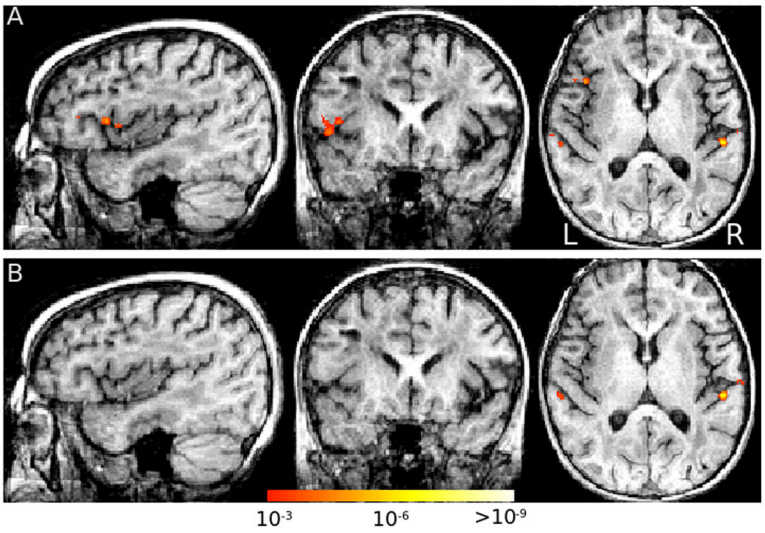

Figure 6.
fMRI to localize language regions. (A) Verb generation vs. rest, showing left inferior frontal gyrus (Broca's area) activation, along with bilateral auditory cortex posteriorly. (B) Auditory noise vs. rest, showing activation of bilateral auditory cortex.

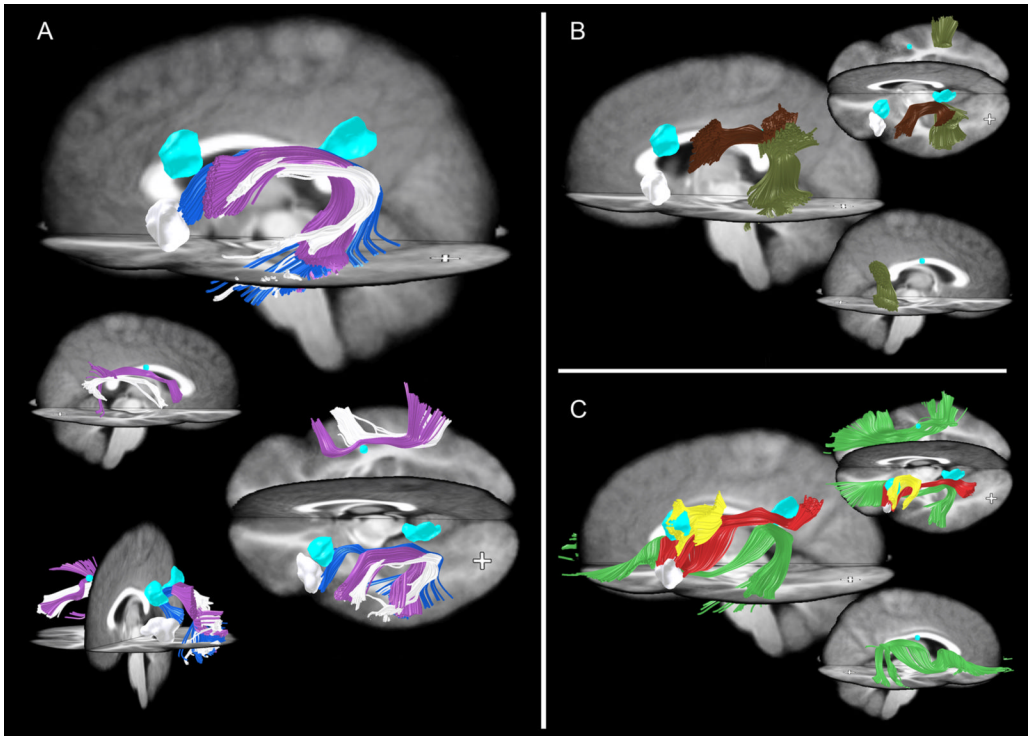

Figure 7.

Pathways not found by tractography in S's brain shown in various views. Cyan-colored ROIs represent cysts in S's brain. White ROI represents S's Broca's area as produced by verb generation during fMRI. Note that although tractography was guided by the results of the statistical test, the findings of missing tracts in S are not dependent in any way on the control group. (A) The "classical arcuate" pathway [blue and purple for controls, see also Catani et al (2005)] is missing in the left and right hemispheres in S. One pathway resembling the shape of the arcuate was found bilaterally in S (white). Note, however, that this pathway connects different regions of cortex than in controls. In the left hemisphere, it does not connect to the left lateral-frontal language region identified in S by verb generation using fMRI (white ROI) and therefore cannot be the arcuate. (B) Indirect arcuate pathways [mahogany, olive; see also Catani et al (2005)] present in controls but not in S. S does have an anterior indirect segment in the right hemisphere (not shown), but is missing the posterior right and anterior and posterior left hemisphere segments. (C) Additional pathways not identified in S. Bilaterally, the normal SLF pathways present in controls (green, red) are not present in S. Additionally in the left hemisphere, a local U-fiber connection (yellow) present in the control group is missing in S. This pathway is positioned in a region where S's brain contains a CSF-filled cyst. We were unable to identify any similar pathways (i.e. connecting these two areas of cortex) in S in the area surrounding the cyst.

Table 1

Pre- and Post-LB Intervention

Tests Administered	9/1999	1999	1/2000	2000	7/2000	2004	2005	9/2005
GORT-3/4*	Form A		Form A		Form A			Form B
Rate (Raw Score)	0		0		0			8
(Percentile)	1		<1		<1			<1
Accuracy (Raw Score)	0		0		0			8
(Percentile)	1		<1		<1			<1
Comprehension (Raw Score)	0		0		7			13
(Percentile)	<1		<1		1			1
WRAT-3	Blue Form		Blue Form		Blue Form			Blue Form
Reading (Raw Score)					23			27
(Percentile)					2			1
Spelling (Raw Score)	17		18		20			
(Percentile)	3		3		5			
WRMT-Revised					Form G			Form G
Word Arrack (Raw Score)					14			19
(Percentile)					20			6

**GORT-3 was administered in 1999, 2000, GORT-4 was administered in 2005.* Raw and age-normed percentile scores are reported for all tests. GORT-3; Gray Oral Reading Test-3, GORT-4; Gray Oral Reading Test-4, WRAT-3; Wide Range Achievement Test-3, WRMT-R; Woodcock Reading Mastery Test-Revised. Shaded bars indicate periods of intervention.

Table 2

Neuropsychological Test Scores

Domains/Tests Administered	2001 11 yrs.		2003 13 yrs.		2006 15 yrs.		2007 16 yrs.	
Intellectual functioning (M=100, SD=15)*	SS**	%ile	SS	%ile	SS	%ile	SS	%ile
Full Scale IQ	78	7	72	3	68	2		
Verbal Comprehension	95	37	89	23	99	47		
Perceptual Reasoning	73	4	65	1	55	<1		
Freedom from Distractibility	61	<1	52	<1				
Working Memory (FD in 2001/2003)					59	<1		
Processing Speed	75	5	91	27	75	5		
Similarities	13	84	9	37	10	50		
Vocabulary	9	37	10	50	10	50		
Block Design	1	<1	1	<1	3	1		
Matrix Reasoning					2	<1		
Digit Span	4	2	1	<1	1	<1		
Letter-Number Sequencing					5	5		
Coding	8	25	6	9	5	5		
Symbol Search	2	<1	10	50	6	9		
Achievement								
WJ-III Subtests								
Letter-Word Identification			55	<1	47	<1		
Reading Fluency			65	1	66	1		
Passage Comprehension			51	<1	49	<1		
Word Attack					69	2		
Calculation			68	2	42	<1		
Spelling			61	<1				
GORT-4 Oral Reading Quotient					55	<1		
TOWRE Total Score					47	<1		
Phonological Processing								
CTOPP Composites								
Phonological Awareness					67	1		

Domains/Tests Administered	2001 11 yrs.	2003 13 yrs.	2006 15 yrs.		2007 16 yrs.	
Phonological Memory			58	<1		
Rapid Naming			49	<1		
Language						
CELF-4						
Word Definitions					13	84
Word Classes 2-Receptive					7	16
Understanding Spoken Paragraphs					9	37
Semantic Relationships					5	5
Recalling Sentences					9	37
Formulated Sentences					7	16
Word Classes 2-Expressive					9	37
Controlled Oral Word Association					6	9
Animal Naming Test					11	63
Boston Naming Test-2					7	16
Executive Function						
WCST # of Categories 6/6						>16
Conceptual Level Responses					15	95
Memory						
WMS-III						
Word List I-Recall Total Score					3	<1
Word List II-Recall Total Score					8	25
Faces I-Recognition					8	25
Faces II-Recognition					6	9
Working Memory						
WMS-III						
Digit Span					4	2
Spatial Span					2	<1

[*] WISC-III was administered in 2001, 2003. WISC-IV was administered in 2006.

[**] Standard or (age-based) scaled scores are reported for all tests, along with the percentile equivalents. Percentile scores of 16 to 24 are within the low average range, percentile scores of 25 to 75 are within the average range, and percentile scores of 76 to 90 are within the high average range. WISC=Wechsler Intelligence Scale for Children, WJ-III=Woodcock-Johnson Tests of Achievement-III, GORT-4, Gray Oral Reading Test-4, TOWRE=Test of Word Reading Efficiency, CTOPP=Comprehensive Test of Phonological Processing, CELF-4=Clinical Evaluation of Language Fundamentals-4, WCST=Wisconsin Card Sorting Test, WMS-III=Wechsler Memory Scale-III.